

# VOVTRACK: EXPLORING THE POTENTIALITY IN VIDEOS FOR OPEN-VOCABULARY OBJECT TRACKING

**Zekun Qian & Wei Feng**

College of Intelligence and Computing, Tianjin University, Tianjin, China

**Ruize Han**

Shenzhen Institute of Advanced Technology, Chinese Academy of Sciences, Shenzhen, China  
City University of Hong Kong, Hong Kong  
rz.han@siat.ac.cn

**Linqi Song & Junhui Hou**

City University of Hong Kong, Hong Kong

## ABSTRACT

Open-vocabulary multi-object tracking (OVMOT) represents a critical new challenge involving the detection and tracking of diverse object categories in videos, encompassing both seen categories (base classes) and unseen categories (novel classes). This issue amalgamates the complexities of open-vocabulary object detection (OVD) and multi-object tracking (MOT). Existing approaches to OVMOT often merge OVD and MOT methodologies as separate modules, predominantly focusing on the problem through an image-centric lens. In this paper, we propose VOVTrack, a novel method that integrates object states relevant to MOT and video-centric training to address this challenge from a video object tracking standpoint. First, we consider the tracking-related state of the objects during tracking and propose a new prompt-guided attention mechanism for more accurate localization and classification (detection) of the time-varying objects. Subsequently, we leverage raw video data without annotations for training by formulating a self-supervised object similarity learning technique to facilitate temporal object association (tracking). Experimental results underscore that VOVTrack outperforms existing methods, establishing itself as a state-of-the-art solution for open-vocabulary tracking task.

## 1 INTRODUCTION

Multi-Object Tracking (MOT) is a fundamental task in computer vision and artificial intelligence, which is widely used for video surveillance, media understanding, *etc.* In the past years, plenty of datasets, *e.g.*, MOT-20 (Dendorfer et al., 2020), DanceTrack (Sun et al., 2022), KITTI (Geiger et al., 2012), as well as the algorithms, *e.g.*, SORT (Wojke et al., 2017), Tractor (Sridhar et al., 2019), FairMOT (Zhang et al., 2021), have been proposed for MOT problem. However, most previous works focus on the tracking of simple object categories, *i.e.*, humans and vehicles. Actually, it is important for the perception of various categories of objects in many real-world applications. Some recent works have begun to study the tracking of generic objects. TAO (Dave et al., 2020) is the first large dataset for the generic MOT, which includes 2,907 videos and 833 object categories. The later GMOT-40 (Bai et al., 2021) includes 10 categories and 40 videos with dense objects in each video.

With the development of Artificial General Intelligence (AGI) and multi-modal foundation models, open-world object perception has become a popular topic. Open-vocabulary object detection (OVD) is a new and promising task because of its generic settings. It aims to identify the various categories of objects from an image, including both the categories that have been seen during training (namely base classes) and not seen (namely novel classes). Although OVD has been studied in a series of works (Dhamija et al., 2020; Joseph et al., 2021; Doan et al., 2024), the literature on open-vocabulary (multi-) object tracking is rare. The nearly sole work (Li et al., 2023) builds a benchmark for

open-vocabulary multi-object tracking (OVMOT) based on TAO (Dave et al., 2020). The authors also develop a simple framework for this problem consisting of a detection head and a tracking head. The detection head is directly taken from an existing OVD algorithm, i.e., DetPro (Du et al., 2022), which is used to detect the open-vocabulary categories of objects in each frame without considering any tracking-related factors. Then the tracking head is used to learn the similarities among the detected objects in different frames. Since the lack of video data with open-vocabulary tracking annotations, the approach in Li et al. (2023) uses a data hallucination strategy to generate the image pairs for training the tracking head. However, the generated image pairs ignore the adjacent continuity and temporal variability of the objects in a video sequence. As discussed above, the existing method for open-vocabulary tracking simply combines the approaches of OVD and MOT in series as independent modules. It does not consider the object states during tracking, e.g., mutual occlusion, motion blur, etc., and does not make use of the sequential information in the videos.

Therefore, in this work, we aim to handle the open-vocabulary object tracking from the standpoint of continuous videos. The comparison between our method and that in Li et al. (2023) can be intuitively seen from Figure 1. Specifically, we first consider the various states of the objects during tracking. Our basic idea is the damaged objects (e.g., with occlusion, motion blur, etc.) should be weakened for foreground object feature learning. This way, we model these states as the prompts, which are used to calculate the attention weights of each generated detection proposal during training the object detection network. This methodology can provide more accurate detection (localization and classification) results of the time-varying objects during tracking. Second, to fully utilize the raw videos without open-vocabulary tracking annotations, we formulate the temporal association (tracking) task as a constraint optimization problem. The basic idea is that each object should maintain consistency across different frames, allowing us to leverage object consistency to effectively learn the object appearance similarity features for temporal association. Specifically, we formulate the object appearance self-consistency as the *intra-consistency*, and the spatial-appearance mutual-consistency as the *inter-consistency* learning problem, in which we also consider the object category consistency. These consistencies work together to learn the object appearance similarity features for the temporal association (tracking) sub-task, thus enhancing the overall performance of OVMOT. Notably, the existing OVMOT dataset TAO provides 534.1K (frames) of unlabeled video data. Compared to the 18.1K annotated samples, the unlabeled ones have a huge potentiality to be explored for training. Our self-supervised training method obtains significant performance improvements only using the raw data thus effectively alleviating the burden of annotations for OVMOT. The main contributions of this work are:

- We propose a new tracking-related prompt-guided attention for the localization and classification (detection) in the open-vocabulary tracking problem. This method takes notice of the states of the time-varying objects during tracking, which is different from the open-vocabulary object detection from a single image.
- We develop a self-supervised object similarity learning strategy for the temporal association (tracking) in the OVMOT problem. This strategy, for the first time, makes full use of the raw video data without annotation for OVMOT training, thus addressing the problem of training data shortage and eliminating the heavy burden of annotation of OVMOT.
- Experimental results on the public benchmark demonstrate that the proposed VOVTrack achieves the best performance with the same training dataset (annotations), and comparable performance with the methods using a large dataset (CC3M) for training.

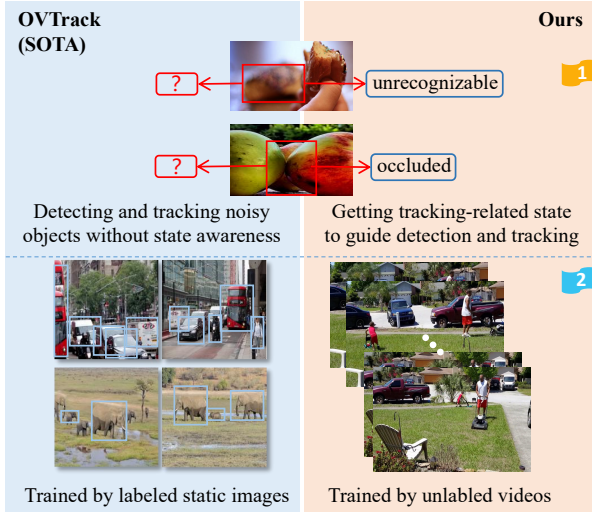


Figure 1: Comparison between prior (Li et al., 2023) and our methods.

## 2 RELATED WORK

**Multiple object tracking.** The prevailing paradigm in MOT is the tracking-by-detection framework (Andriluka et al., 2008), which involves detecting objects in each frame first, and then associating objects across different frames using various cues such as object appearance features (Bergmann et al., 2019; Fischer et al., 2023; Leal-Taixé et al., 2016; Milan et al., 2017; Pang et al., 2021; Sadeghian et al., 2017; Wojke et al., 2017; Cai et al., 2022), 2D motion features (Zhou et al., 2020; Saleh et al., 2021; Xiao et al., 2018; Qin et al., 2023; Du et al., 2023), or 3D motion features (Huang et al., 2023; Luiten et al., 2020; Wang et al., 2023; Krejčí et al., 2024; Ošep et al., 2018; Sharma et al., 2018b). Some methods leverage graph neural networks (Bochinski et al., 2017; Ding et al., 2023) or transformers (Meinhardt et al., 2022; Sun et al., 2020; Zeng et al., 2022; Zhou et al., 2022d) to learn the association relationships between objects, thereby enhancing tracking performance. To broaden the object categories of the MOT task, the TAO benchmark (Dave et al., 2020) has been proposed for studying MOT under the long-tail distribution of object categories. On this benchmark, relevant methods include AOA (Du et al., 2021), GTR (Zhou et al., 2022d), TET (Li et al., 2022), QDTrack (Fischer et al., 2023), *etc.* While these methods perform well, they are still limited to pre-defined object categories, which makes them unsuitable for diverse open-world scenarios. Differently, this work handles OVMOT problem, which contains categories not seen during training.

**Open-world/vocabulary object detection.** Unlike traditional object detection with closed-set categories that appear at the training time. The task of open-world object detection aims to detect salient objects in an image without considering their specific categories (Dhamija et al., 2020; Joseph et al., 2021; Doan et al., 2024). This allows the method to detect objects of categories beyond those present in the training set. However, such methods do not classify objects into specific categories and only regard the object classification task as a clustering task (Joseph et al., 2021), achieving classification by calculating the similarity between objects and different class clusters. Consistent with the objective of open-world detection, open-vocabulary object detection requires the identification of categories not seen in the training set. However, unlike open-world detection, open-vocabulary object detection needs to predict the specific object categories (Zareian et al., 2021). To achieve this, some works (Bansal et al., 2018; Rahman et al., 2020) train the detector with text embeddings. Recently, pre-trained vision-language models, *e.g.*, CLIP (Radford et al., 2021) connect visual concepts with textual descriptions, which has a strong open-vocabulary classification ability to classify an image with arbitrary categories described by language. Based on this, many works (Gu et al., 2022; Zhou et al., 2022c; Wu et al., 2023) utilize pre-trained vision-language models to achieve open-vocabulary object detection and few-shot object detection. In addition, some studies (Du et al., 2022; Zhou et al., 2022a;b) further enhance the effectiveness of prompt embeddings of class descriptions using prompt learning methods, thereby improving the results of open-vocabulary detection. Different from the above detection methods developed for single image, in this work, we propose a prompt-guided training method designed for open-vocabulary detection in continues videos, which can effectively enhance the detection performance for the video tracking task.

**Open-world/vocabulary object tracking.** There are relatively few works addressing the task of open-world tracking. Related approaches aim to segment or track all the moved objects in the video (Mitzel & Leibe, 2012; Dave et al., 2019) or handle the generic object tracking (Ošep et al., 2016; 2018; 2020) using a class-agnostic detector. Recently, the TAO-OW benchmark (Liu et al., 2022) is proposed to study open-world tracking problems, but its limitation lies in evaluating only class-agnostic tracking metrics without assessing class-related metrics. To make the setting more practical, OVTrack (Li et al., 2023) first brings the setting of open vocabulary into the tracking task, which also develops a baseline method and benchmark based on the TAO dataset. However, the method in Li et al. (2023) directly uses an existing OVD algorithm for detection, and its training process only utilizes static image pairs and ignores the information from video sequences. Differently, we consider the tracking-related object states for detection, and also propose a self-supervised video-based training method designed for open-vocabulary tracking, making full use of video-level information to enhance the performance of open-vocabulary tracking.

### 3 PROPOSED METHOD

#### 3.1 OVERVIEW AND VOVTRACK FRAMEWORK

OVMOT requires localizing, tracking, and recognizing the objects in a video, whose problem formulation is provided in Appendix 1. We first describe the framework of our VOVTrack, which mainly includes the object localization, object classification, and temporal association modules, as shown in Figure 2. For improving the localization and classification, in Section 3.2, we design a tracking-state-aware prompt-guided attention mechanism, which can help the network learn more effective object detection features. For learning the temporal association similarity, in Section 3.3, we propose a video-based self-supervised method to train the association network, which considers the appearance intra-/inter-consistency and category consistency, to enhance the tracking performance.

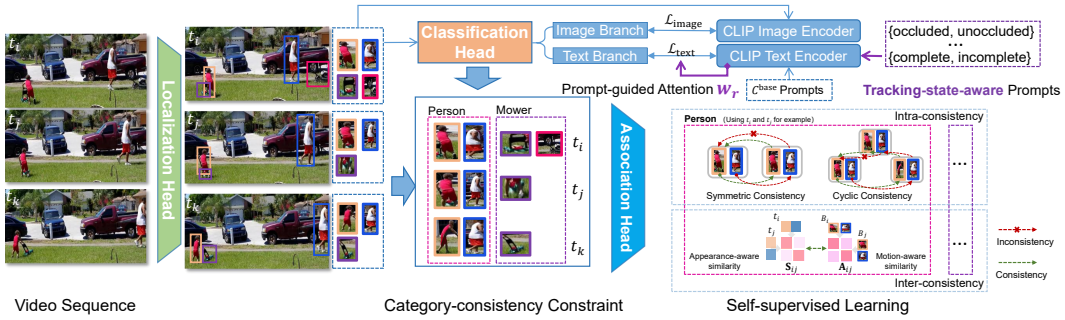


Figure 2: Training framework consists of three parts: first is the localization head used to localize objects of all categories in the video as region candidates; the second is the CLIP distilled classification head consisting of image and text branches, which uses tracking-state-aware prompts to guide the model in focusing on object states while learning classification features, thereby better distinguishing the OV categories; and the third part is the association head that utilizes intra/inter-consistency between the same objects in different frames to learn association features in a self-supervised way.

**Localization:** We employ the class-agnostic object proposal generation approach in Faster R-CNN (Ren et al., 2015) to localize objects for both base and novel categories  $\mathcal{C}$  in the video. As supported by prior researches (Dave et al., 2019; Gu et al., 2022; Zhou et al., 2022c; Li et al., 2023), the localization strategy has shown robust generalization capabilities towards the novel object class  $\mathcal{C}^{novel}$ . During the training phase, we leverage the above-mentioned generated RPN proposals as the initial object candidates  $P$ . The localization result of each candidate  $r \in P$  is the bounding box  $\mathbf{b} \in \mathbb{R}^4$ . For each  $\mathbf{b}$ , we also obtain a confidence  $p_c \in \mathbb{R}$  derived from the classification head. To refine the localization candidates, besides the classical non-maximum suppression (NMS), we also use this confidence  $p_c$ . For a more effective  $p_c \in \mathbb{R}$  in the classification head, we use a prompt-guided attention strategy, which will be discussed in later Section 3.2.

**Classification:** Existing closed-set MOT trackers only track several specific categories of objects, which do not need to provide the class of each tracked object. This way, classification is a new sub-task of the OVMOT. To enable the framework to classify open-vocabulary object classes, following the OV detection algorithms (Gu et al., 2022; Zhou et al., 2022c; Wu et al., 2023), we leverage the knowledge from the pre-trained model, *i.e.*, CLIP (Radford et al., 2021), to help the network recognize objects belonging to the novel classes  $\mathcal{C}^{novel}$ . We distill the classification head using the CLIP model to empower the network’s classification head to recognize new objects. Specifically, as shown in Figure 2, after obtaining the RoI feature embeddings  $\mathbf{f}_r$  from the localization head, we design the classification head with a text branch and an image branch to generate embeddings  $\mathbf{f}_r^{text}$  and  $\mathbf{f}_r^{img}$  for each  $\mathbf{f}_r$ . The supervisions of these heads are generated by the CLIP text and image embeddings. We use the method in Du et al. (2022) for CLIP encoder pre-training.

First, we align the text branch with the CLIP text encoder. For  $\forall c \in \mathcal{C}^{base}$ , the class text embedding  $\mathbf{t}_c$  of class  $c$  can be generated by the CLIP text encoder  $\mathcal{T}(\cdot)$  as  $\mathbf{t}_c = \mathcal{T}(c)$ . We compute the affinity

between the predicted text embeddings  $\mathbf{f}_r^{\text{text}}$  and their CLIP counterpart  $\mathbf{t}_c$  as

$$\begin{aligned} z(r) &= [\cos(\mathbf{f}_r^{\text{text}}, \mathbf{t}_{\text{bg}}), \cos(\mathbf{f}_r^{\text{text}}, \mathbf{t}_1), \dots, \cos(\mathbf{f}_r^{\text{text}}, \mathbf{t}_{|C^{\text{base}}|})], \\ \mathcal{L}_{\text{text}} &= \frac{1}{|P|} \sum_{r \in P} w_r \text{L}_{\text{CE}} \left( \text{softmax} \left( \frac{z(r)}{\lambda}, c_r \right) \right), \end{aligned} \quad (1)$$

where  $\mathbf{t}_{\text{bg}}$  is a background prompt learned by treating the background candidates as a new class,  $w_r$  is the tracking-related prompt-guided attention weight (described in Section 3.2),  $\lambda$  is a temperature parameter,  $\text{L}_{\text{CE}}$  is the cross-entropy loss and  $c_r$  is the class label of  $r$ .

Then, we align each image branch embedding  $\mathbf{f}_r^{\text{img}}$  with the CLIP image encoder  $\mathcal{I}(\cdot)$ . For each candidate object  $r$ , we input the corresponding cropped image to  $\mathcal{I}(\cdot)$  and get the CLIP image embedding  $\mathbf{i}_r$ . We minimize the distance between the corresponding  $\mathbf{f}_r^{\text{img}}$  and  $\mathbf{i}_r$  as

$$\mathcal{L}_{\text{image}} = \frac{1}{|P|} \sum_{r \in P} \|\mathbf{f}_r^{\text{img}} - \mathbf{i}_r\|. \quad (2)$$

In the testing stage, with the embeddings  $\mathbf{f}_r^{\text{text}}$  and  $\mathbf{f}_r^{\text{img}}$  derived from the text branch and image branch, respectively, we can obtain the corresponding classification probabilities  $p_c^{\text{text}}$  and  $p_c^{\text{img}}$  of each  $r$  belonging to the class  $c$ , using the  $z(r)$  and softmax operation in Eq. (1). After that, we use the fusion strategy in Gu et al. (2022) to calculate the final classification probability  $p_c$ .

**Association:** The association head is to associate the detected objects with the same identification across frames, the main purpose of which is to learn the object features for similarity measurement.

In the training stage, given the detected objects from the localization head, we use the appearance embedding to extract the features for association. For training the appearance embedding model, a straightforward method is to select an object as the anchor, and its positive/negative samples for learning the object similarity. This method requires object identification (ID) annotations for positive/negative sample selection. However, as an emerging problem, OVMOT does not have enough available training video datasets with tracking ID labels. Previous work (Li et al., 2023) uses data augmentation to generate the image pairs for training the association head, which, however, ignores the temporal information in the videos. In this work, we propose to leverage the *unlabeled videos* to train the association network in a *self-supervised strategy*, which will be discussed in Section 3.3.

In the inference stage, we use appearance feature similarity to associate history tracks with the objects in the current frame. As in Li et al. (2023), we evaluate the similarity between history tracks and detected objects using both bi-directional softmax (Fischer et al., 2023) and cosine similarity metrics. Following the classical MOT approaches, if the similarity score exceeds a matching threshold, we assign the object to the track. If the object doesn't correspond to any existing track, a new track is initiated if its detection confidence score surpasses a threshold, otherwise, it is disregarded.

### 3.2 TRACKING-STATE-AWARE PROMPT GUIDED ATTENTION

**Tracking-state-aware prompt.** In the classification head of existing open-vocabulary detection methods, when selecting region candidates for calculating classification loss, they only consider whether the maximal IOU between the candidates and ground-truth box exceeds a threshold. For this tracking problem, we further consider whether the states of the candidates are appropriate for training the detection network.

As is well known, the objects present many specific states during tracking, such as occlusion/out-of-view/motion blur, *etc.*, which are more frequent than the object detection in static images. So, it is important to identify such object states to achieve more accurate detection and tracking results. However, these states have often been overlooked in past methods because the labels of these states are difficult to obtain, not to mention incorporating them into the network training.

Prompt, as a burgeoning concept, can be used to bridge the gap between the vision and language data based on the cross-modal pre-trained models. We consider using specially designed prompts to perceive the tracking states of the objects and integrate such states into the model training. We refer to such prompts as 'tracking-state-aware prompts'. We specifically employ pairs of adjectives with opposite meanings to describe the object states during tracking. For example, 'unoccluded and occluded'. As shown in classification head of Figure 2, we add  $M$  pairs of tracking-state-aware



prompt pairs, denoted as  $\{p_{\text{pos}}^m, p_{\text{neg}}^m\}_{m=1}^M$ , into ore framework model. Next, we present how to use these promotes during training.

**Prompt-guided attention.** To utilize these tracking-state-aware prompts guiding model training, we encode these prompts through the CLIP text encoder  $\mathcal{T}(\cdot)$  to obtain state embeddings  $\{\mathbf{t}_{\text{pos}}^m, \mathbf{t}_{\text{neg}}^m\}_{m=1}^M$ , and calculate the prompt-guided attention weight  $w_r$  as

$$z(r, m) = [\cos(\mathbf{f}_r^{\text{text}}, \mathbf{t}_{\text{pos}}^m), \cos(\mathbf{f}_r^{\text{text}}, \mathbf{t}_{\text{neg}}^m)], \quad w_r = \frac{1}{|M|} \sum_{m=1}^M \left( \text{softmax} \frac{z(r, m)}{\lambda} \right)_1, \quad (3)$$

where  $\mathbf{f}_r^{\text{text}}$  is the text embedding of a region candidate  $r$ , and  $(\cdot)_1$  represents using the probability of the positive state as the attention for this pair. Note that, in our definition, the positive states always denote that the object state is beneficial to the object feature learning, *e.g.*, unoccluded, unobscured. From the above analysis, we know that the attention obtained from the tracking-state-aware prompts evaluates the various object states, resulting in prompt-guided attention values  $w_r \subseteq [0, 1]$ .

**Piecewise weighting strategy.** Next, we use this prompt-guided attention to help the model better utilize high-quality candidates for training and filter out the low-quality noisy candidates. Specifically, we divide the  $w_r$  into three levels: low ( $d_{\text{low}}$ ), medium and high ( $d_{\text{high}}$ ). For embedding features  $\mathbf{f}_r^{\text{text}}$  with  $w_r < d_{\text{low}}$ , we regard such features as low-quality state, and filter them out during training, by assigning  $w_r$  to 0. For  $d_{\text{low}} \leq w_r \leq d_{\text{high}}$ , we regard that even if these features are not of high quality, they still contribute to training, and retain their original weights  $w_r$ . For  $w_r > d_{\text{high}}$ , we regard the features of these regions as particularly suitable ones for the model to learn tracking-related features, so we assign  $w_r$  to 1 as an award. After that, we apply the re-assigned  $w_r$  to Eq. (1), thereby integrating the object tracking-related state into the model training, which enables the network to better learn the object representations specifically for the tracking task.

### 3.3 SELF-SUPERVISED OBJECT ASSOCIATION WITH RAW VIDEO DATA

Considering the lack of annotated videos for OVMOT, we develop a self-supervised approach to train the association network by leveraging the consistency among the same objects during a video.

#### 3.3.1 FORMULATION

**Objective function.** To learn the object appearance feature, we consider two aspects. The first one is **intra factor**, *i.e.*, the self-consistency of appearance for the same object at different times. The second one is **inter factor**, *i.e.*, the mutual-consistency between the appearance and motion cues during tracking. This way, we formulate the optimized objective function as

$$\max S = S_{\text{intra}}(t_i, t_j) + \alpha \cdot S_{\text{inter}}(t_i, t_j), \quad \text{s.t.} \quad \forall t_i, t_j \in \mathcal{T}_c, \quad \forall c \in \mathcal{C}, \quad (4)$$

where  $S$  represents the overall consistency objective to be maximized,  $S_{\text{intra}}$  and  $S_{\text{inter}}$  denote the intra and inter consistency measures respectively, while  $\alpha$  is a weight to balance them. Besides, considering the diversity of object categories in the OVMOT problem, we add the object category consistency constraint for the consistency learning. Specifically, we construct the intervals, *e.g.*,  $\mathcal{T}_c$ , which contain several frames only with the same object category  $c$ , in which we select  $t_i, t_j$ . This is because we aim to learn the feature in a self-supervised manner without ID annotation, the objects with various categories may bring about interference.

**Long-short-interval sampling.** First, we consider the interval splitting of  $\mathcal{T}_c$  in Eq. (4). We split the original videos into several segments of length  $L$  and randomly sample the shorter sub-segments with various lengths from each segment. These short-term sub-segments are then concatenated to form the training sequence. Such training sequences include long-short-term intervals. Specifically, we select the adjacent frames from the same sub-segment, which allow the association head to learn the consistency objectives under minor object differences. We also select the long-interval video frames from different sub-segments, which allow the association head to learn the similarity and variation of objects under large differences.

**Category-consistency constraint.** Then we consider the category consistency constraint in  $\mathcal{T}_c$ . After obtaining the sampled training sequences as discussed above, we utilize the localization head to extract object bounding boxes from each frame in the sequence. Since we only use unlabeled

raw videos for training, we cannot directly obtain the object categories. To address this issue, we employ a clustering approach to group the bounding boxes based on their classification features. Specifically, we utilize the classification head to obtain the category features for the candidate objects from all frames. Then we cluster the candidate objects’ category features as different clusters. After clustering the candidate objects’ category features into distinct groups, we can treat each cluster as a separate category. As illustrated in Figure 2, we proceed to conduct self-supervised learning on the objects that belong to the same category cluster and are sourced from different frames.

### 3.3.2 SELF-SUPERVISED LOSS CONSTRUCTION

We next model the consistency learning problem in Eq. (4) as a self-supervised learning task.

**Intra-consistency loss.** After getting the training samples (object bounding boxes in different frames of the sample training sequence within the category clustering), we first use the CNN network to extract the appearance feature from the association head for all objects in frame  $t_i$  to construct the feature matrix  $\mathbf{F}_i$ . The main idea of the intra-consistency loss is to leverage the self-consistency of the same objects at different times (frames). We utilize the following two types of similarity transfer relationships, *i.e.*, pair-wise symmetry and triple-wise cyclicity.

- *Consistent learning from the symmetry:* For a pair of frames  $t_i$  and  $t_j$  in the video, we can get the object similarity matrix between them as

$$\mathbf{M}_{ij} = \mathbf{F}_i \cdot (\mathbf{F}_j)^T. \quad (5)$$

We then compute the *normalized similarity matrix*  $\mathbf{S}_{ij} \in [0, 1]$  based on the above similarity matrix  $\mathbf{M}_{ij}$  by temperature-adaptive row softmax as

$$\mathbf{S}(r, c) = f_{r,c}(\mathbf{M}) = \frac{\exp(\tau \mathbf{M}(r, c))}{\sum_{c=1}^C \exp(\tau \mathbf{M}(r, c))} \quad (6)$$

where  $r, c$  represent the indices of row and column in  $\mathbf{M}$ , respectively. Here  $C$  is the number of columns for  $\mathbf{M}$ , and  $\tau$  is the adaptive temperature adjustable parameter.

The normalized similarity matrix  $\mathbf{S}_{ij}$  can be regarded as a mapping (object association relation) from frame  $t_i$  to frame  $t_j$  ( $\mathbf{S}_{ij} : t_i \rightarrow t_j$ ). In other words, we can select the maximum value of each row of  $\mathbf{S}$  as the matched objects between frames  $t_i$  and  $t_j$ . Similarly, we get the reversed mapping from  $t_j$  to  $t_i$  as  $\mathbf{S}_{ji} : t_j \rightarrow t_i$ . We calculate the pair-wise symmetric-similarity matrix as  $\mathbf{E}_{\text{pair}} = \mathbf{S}_{ij} \cdot \mathbf{S}_{ji}$ , where  $\mathbf{E}_{\text{pair}}$  can be regarded as a symmetric mapping:  $t_i \rightleftharpoons t_j$ , *i.e.*, from  $t_i$  and return  $t_i$ . If the objects in frames  $t_i$  and  $t_j$  are the same, the result  $\mathbf{E}_{\text{pair}}$  should be an identity matrix, which can be used to construct the self-supervision loss. However, due to the object differences in different frames, this condition may not be always satisfied. Therefore, we need to supervise it deliberately, which will be discussed later.

- *Consistent learning from the cyclicity:* Besides the pair-wise symmetric similarity, we further consider the triple-wise circularly consistent similarity. Specifically, given the similarity matrix  $\mathbf{S}_{ij}$  between two frames  $t_i$  and  $t_j$ , as well as  $\mathbf{S}_{jk}$  between frames  $t_j$  and  $t_k$ , we aim to build the consistent similarity relation among this triplet, *i.e.*, frames  $t_i, t_j$  and  $t_k$ . To do this, we first calculate the third-order similarity matrix as

$$\mathbf{M}_{ik} = \mathbf{M}_{ij} \cdot \mathbf{M}_{jk}, (i \neq j \neq k), \quad (7)$$

where  $\mathbf{M}_{ik}$  represents the similarity between the objects in frames  $t_i$  and  $t_k$ , through the frame  $t_j$ . We then compute the normalized similarity matrix using Eq. (6) as

$$\mathbf{S}_{ik} = f(\mathbf{M}_{ik}), \quad \mathbf{S}_{ki} = f((\mathbf{M}_{ik})^T), \quad (8)$$

where  $\mathbf{S}_{ik}$  represents the mapping  $t_i \rightarrow t_j \rightarrow t_k$  while  $\mathbf{S}_{ki}$  represents the mapping along  $t_k \rightarrow t_j \rightarrow t_i$ . Then, we calculate the transitive-similarity matrix:  $\mathbf{E}_{\text{trip}} = \mathbf{S}_{ik} \cdot \mathbf{S}_{ki}$ , where  $\mathbf{E}_{\text{tri}}$  can be regarded as the mapping:  $t_i \rightleftharpoons t_j \rightleftharpoons t_k$  (from  $t_i$  and return  $t_i$ ).

For convenience, we note the matrices  $\mathbf{E}_{\text{pair}}$  and  $\mathbf{E}_{\text{trip}}$  as  $\mathbf{E}$ , which should have the property that their diagonal elements are either 1 or 0, while all other elements are 0, in an ideal case. This means that the diagonal elements of  $\mathbf{E}$  must be greater than or equal to the other elements. Based on this consideration, following Wang et al. (2020); Feng et al. (2024), we use the following loss  $L(\mathbf{E}) = \sum_r \text{relu}(\max_{c \neq r} \mathbf{E}(r, c) - \mathbf{E}(r, r) + m)$ , where  $r, c$  denote the indices of row and column

in  $\mathbf{E}$ . This loss denotes that we penalize the cases where the max non-diagonal element  $\mathbf{E}(r, c)$  ( $c \neq r$ ) in a row  $r$ , exceeds the corresponding diagonal elements  $\mathbf{E}(r, r)$  with a margin  $m$ . The margin  $m \geq 0$  is a parameter used to control the punishment scope between  $\mathbf{E}(r, c)$  and  $\mathbf{E}(r, r)$ . This loss helps  $\mathbf{E}$  approach the identity matrix while addressing cases where there are unmatched targets in a row through a margin  $m$ . Finally, we define our self-supervised consistency learning loss (intra) as  $\mathcal{L}_{\text{intra}} = \mathcal{L}(\mathbf{E}_{\text{pair}}) + \mathcal{L}(\mathbf{E}_{\text{trip}})$ .

**Inter-consistency loss.** The inter-consistency loss makes use of the consistency between the spatial position continuity and the appearance similarity of the objects at different times. Given a bounding box list  $B_i$  and  $B_j$  of adjacent frames  $i$  and  $j$  in the video, we compute the Intersection over Union (IoU) matrix  $\mathbf{M}_{ij}$  between bounding boxes  $B_i$  and  $B_j$ , which quantifies the overlap between them. Based on a specified threshold  $\text{IoU}_{\text{thres}}$ , we create an assignment matrix  $\mathbf{A}_{ij}$  such that

$$\mathbf{A}_{ij} = \begin{cases} 1 & \text{if } \mathbf{M}_{ij} > \text{IoU}_{\text{thres}} \\ 0 & \text{otherwise} \end{cases}, \quad (9)$$

This assignment matrix  $\mathbf{A}_{ij}$  indicates whether pairs of objects are considered similar, facilitating the optimization of the spatial consistency objective. Furthermore, we utilize the previously obtained normalized similarity matrix  $\mathbf{S}_{ij}$  to establish the inter-consistency loss, using the binary cross-entropy loss function  $\mathcal{L}_{\text{BCE}}$ , as  $\mathcal{L}_{\text{inter}} = \mathcal{L}_{\text{BCE}}(\mathbf{S}_{ij}, \mathbf{A}_{ij})$ . This formulation allows us to measure the discrepancy between the normalized similarity matrix  $\mathbf{S}_{ij}$  and the assignment matrix  $\mathbf{A}_{ij}$ , thereby enforcing spatial consistency across the detected objects in frames  $t_i$  and  $t_j$ .

Finally, we have transformed the optimization problem in Eq. (4) into a self-supervised loss as  $\mathcal{L} = \mathcal{L}_{\text{intra}} + \alpha \cdot \mathcal{L}_{\text{inter}}$ , where  $\alpha$  is a weighting coefficient. This formulation incorporates both the intra- and inter-consistencies, as well as category consistency, among the frames with different intervals, thereby effectively exploring the potentiality of videos to enhance the association for OVMOT.

### 3.4 IMPLEMENTATION DETAILS

In Section 3.1, we use ResNet50 with FPN for localizing candidate regions. We set  $\lambda$  in Eq. (1) as 0.007. In Section 3.2, we select four pairs of typical tracking state aware prompts, *i.e.*, ‘complete and incomplete’, ‘unoccluded and occluded’, ‘unobscured and obscured’, and ‘recognizable and unrecognizable’. We set  $d_{\text{low}}$  as 0.3,  $d_{\text{high}}$  as 0.6. In Section 3.3, the segment length  $L$  is set as 24. We use the clustering algorithm of K-means. We set the margin  $m$  as 0.5 and the  $\text{IoU}_{\text{thres}}$  as 0.9. For  $N$  frames in each sampled video sequence, we select  $C_N^2$  and  $C_N^3$  groups of frames to calculate the matrices in Eqs. (5) and (7). We also select  $C_N^2$  groups of frames to calculate the inter-consistency loss. The weighting coefficients  $\alpha$  is 0.9.

In the training stage, we first train the two-stage detector on the base classes of LVIS dataset (Gupta et al., 2019) referenced from Du et al. (2022), for 20 epochs, and use prompt-guided attention proposed in Section 3.2 to fine-tune the model’s classification head for 6 epochs. Then we train the association head using static image pairs generated from Li et al. (2023) for 6 epochs and self-supervise the association head with TAO training dataset (Dave et al., 2020) without annotation for 14 epochs. In the inference stage, we select object candidates  $P$  by NMS with IoU threshold 0.5. Additionally, we set the similarity score threshold as 0.35 and maintain a track memory of 10 frames.

## 4 EXPERIMENTS

### 4.1 DATASET AND METRICS

We follow Li et al. (2023) to select the dataset and metrics for evaluation. We leverage the comprehensive and extensive vocabulary MOT dataset TAO (Dave et al., 2020) as our benchmark for OVMOT. TAO is structured similarly to the LVIS (Gupta et al., 2019) taxonomy, categorizing object classes based on their frequency of appearance into frequent, common, and rare groups. We use the rare classes defined in LVIS as  $\mathcal{C}^{\text{novel}}$  and others as  $\mathcal{C}^{\text{base}}$ . We evaluate the performance with the comprehensive metric tracking-every-thing accuracy (TETA), which consists of the accuracies of localization (LocA), classification (ClsA), and association (AssocA).



## 4.2 COMPARATIVE RESULTS

We compare our method with the latest trackers, TETer (Li et al., 2022) and QDTrack (Fischer et al., 2023), which are trained on both  $\mathcal{C}^{\text{base}}$  and  $\mathcal{C}^{\text{novel}}$ . We include the classical trackers like DeepSORT (Wojke et al., 2017) and Tracktor++ (Bergmann et al., 2019) trained only on  $\mathcal{C}^{\text{base}}$  and enhanced by OVD method ViLD (Gu et al., 2022) to achieve open-vocabulary tracking, as baselines. We also compare our method with the state-of-the-art OVMOT method, OVTrack (Li et al., 2023). Besides, following Li et al. (2023), we compare with the existing trackers (DeepSORT, Tracktor++, OVTrack) equipped with the powerful OVD method, *i.e.*, RegionCLIP (Zhong et al., 2022) trained on the extensive CC3M (Sharma et al., 2018a) dataset.

As shown in Table 1, we present the OVMOT evaluation results on the TAO validation and test sets, divided into base classes  $\mathcal{C}^{\text{base}}$  and novel classes  $\mathcal{C}^{\text{novel}}$ . We can see that our method outperforms all closed-set and open-vocabulary methods on both the validation and test sets. Even though QDTrack (Fischer et al., 2023) and TETer (Li et al., 2022) have seen novel classes during training on TAO, our method significantly outperforms them in all metrics on both base and novel classes.

Table 1: Result comparison. We evaluate our method against closed-set and open-vocabulary trackers on TAO validation and test sets. Here ‘✓’ denotes using the corresponding dataset with annotations, and ‘†’ represents only using the raw video without any annotation.

Method	Classes		Data			Base				Novel			
	Base	Novel	CC3M	LVIS	TAO	TETA	LocA	AssocA	ClsA	TETA	LocA	AssocA	ClsA
<b>Validation set</b>													
QDTrack (Fischer et al., 2023)	✓	✓	-	✓	✓	27.1	45.6	24.7	11.0	22.5	42.7	24.4	0.4
TETer (Li et al., 2022)	✓	✓	-	✓	✓	30.3	47.4	31.6	12.1	25.7	45.9	31.1	0.2
DeepSORT (ViLD) (Wojke et al., 2017)	✓	-	-	✓	✓	26.9	47.1	15.8	17.7	21.1	46.4	14.7	2.3
Tracktor++ (ViLD) (Bergmann et al., 2019)	✓	-	-	✓	✓	28.3	47.4	20.5	17.0	22.7	46.7	19.3	2.2
DeepSORT + RegionCLIP*	✓	-	✓	✓	✓	28.4	52.5	15.6	17.0	24.5	49.2	15.3	9.0
Tracktor++ + RegionCLIP*	✓	-	✓	✓	✓	29.6	52.4	19.6	16.9	25.7	50.1	18.9	8.1
OVTrack (Li et al., 2023)	✓	-	-	✓	-	35.5	49.3	36.9	<b>20.2</b>	27.8	48.8	33.6	1.5
OVTrack + RegionCLIP*	✓	-	✓	✓	-	36.3	53.9	36.3	18.7	32.0	51.4	33.2	<b>11.4</b>
VOVTrack (Ours)	✓	-	-	✓	†	<b>38.1</b>	<b>58.1</b>	<b>38.8</b>	17.5	<b>34.4</b>	<b>57.9</b>	<b>39.2</b>	6.0
<b>Test set</b>													
QDTrack (Fischer et al., 2023)	✓	✓	-	✓	✓	25.8	43.2	23.5	10.6	20.2	39.7	20.9	0.2
TETer (Li et al., 2022)	✓	✓	-	✓	✓	29.2	44.0	30.4	10.7	21.7	39.1	25.9	0.0
DeepSORT (ViLD) (Wojke et al., 2017)	✓	-	-	✓	✓	24.5	43.8	14.6	15.2	17.2	38.4	11.6	1.7
Tracktor++ (ViLD) (Bergmann et al., 2019)	✓	-	-	✓	✓	26.0	44.1	19.0	14.8	18.0	39.0	13.4	1.7
DeepSORT + RegionCLIP*	✓	-	✓	✓	✓	27.0	49.8	15.1	16.1	18.7	41.8	9.1	5.2
Tracktor++ + RegionCLIP*	✓	-	✓	✓	✓	28.0	49.4	18.8	15.7	20.0	42.4	12.0	5.7
OVTrack (Li et al., 2023)	✓	-	-	✓	-	32.6	45.6	35.4	16.9	24.1	41.8	28.7	1.8
OVTrack + RegionCLIP*	✓	-	✓	✓	-	34.8	51.1	36.1	<b>17.3</b>	25.7	44.8	26.2	<b>6.1</b>
VOVTrack (Ours)	✓	-	-	✓	†	<b>37.0</b>	<b>56.1</b>	<b>39.3</b>	15.5	<b>29.4</b>	<b>52.4</b>	<b>31.2</b>	4.5

\*Note that, except the RegionCLIP (Zhong et al., 2022), all other methods (including ‘Ours’) use ResNet50 as backbone. Additionally, DeepSORT and Tracktor++ with the open-vocabulary detector ViLD (Gu et al., 2022) are also trained in a supervised manner on TAO, while our method, trained in a self-supervised manner on TAO, surpasses them by a large margin. Although the results of OVTrack, the most competitive method, are better than other comparison methods, our method outperforms it in almost all metrics significantly on both base and novel classes.

Particularly, compared to our baseline method OVTrack, Our method achieves improvements of 2.6% and 6.6% in base and novel TETA, respectively, and a 4.5% increase in novel ClsA. In the test set, base and novel TETA also show improvements of 4.4% and 5.3%, respectively. It is worth noting that even though RegionCLIP-related methods use an additional 3 million image data in CC3M for training, our method outperforms them in almost all metrics, with only ClsA slightly lower. This demonstrates the effectiveness of the proposed approach, which is very promising for the OVMOT task. We provide more analysis from the standpoint of data quantity for training in Appendix 2.

## 4.3 ABLATION STUDY

In this section, we conduct the ablation studies on all components proposed in our method, including the ablation of prompt-guided attention, and the self-supervised learning related modules as:

- w/o prompt-guided attention ( $w_r$ ): Removing the prompt-guided attention in Section 3.2.
- w/o piecewise weight strategy ( $d_{\text{low}}$  and  $d_{\text{high}}$ ): Removing the piecewise weighting strategy proposed in Section 3.2, by directly using the  $w_r$  calculated by Eq. (3).
- w/o self-supervised learning: Removing the whole self-supervised learning strategy in Section 3.3.
- w/o short-long-sampling: Removing the short-long-interval sampling strategy in Section 3.3.
- w/o category consistency: Removing the category-aware object clustering in Section 3.3.

Table 2: Ablation studies on modules of prompt-guided attention and self-supervised association.

Module	Ablation Methods	Base				Novel			
		TETA	LocA	AssocA	ClsA	TETA	LocA	AssocA	ClsA
Prompt-guided attention	w/o prompt-guided attention	35.7	52.7	37.2	17.3	29.8	52.8	34.9	1.7
	w/o piecewise weight strategy	36.3	53.9	37.5	17.4	31.7	53.8	36.8	4.5
Self-supervised association	w/o self-supervised learning	36.3	55.5	36.4	17.1	31.3	55.1	34.7	4.0
	w/o short-long-sampling	37.3	57.2	36.9	<b>17.7</b>	33.1	56.9	37.2	5.1
	w/o category consistency	37.1	57.6	37.4	16.3	32.2	56.0	37.0	3.7
	w/o intra-consistency	37.0	57.0	36.7	17.4	32.3	56.1	36.0	4.9
	w/o inter-consistency	37.2	56.8	37.2	17.6	33.0	56.6	36.8	5.5
	VOVTrack (Ours)	<b>38.1</b>	<b>58.1</b>	<b>38.8</b>	17.5	<b>34.4</b>	<b>57.9</b>	<b>39.2</b>	<b>6.0</b>

- w/o intra-consistency: Removing the intra-consistency consistency loss.
- w/o inter-consistency: Removing the inter-consistency loss in Section 3.3.

**Effectiveness of the state-aware prompt guided attention.** As shown in the first unit of Table 2, we can see that using prompt-guided attention as a weight coefficient during the training stage can effectively improve all metrics for both base and novel classes. The piecewise weighting strategy is also very effective, especially in improving the classification accuracy of novel classes.

**Effectiveness of the self-supervised consistent learning.** As shown in the second unit of Table 2, we can see that using self-supervised loss can effectively improve all metrics for both base and novel classes. Either the intra-consistency or the inter-consistency for appearance learning is effective for the association task, *i.e.*, ‘AssocA’. Also, the interval sampling strategy allows samples to have a more diverse range of long and short cycles, improving the association-related metric. The category clustering strategy tries to gather the objects with the same category in a cluster, which is also helpful. To our surprise, the above strategies, in most cases, also effectively help improve classification (‘ClsA’) and localization (‘LocA’) accuracies. This is because the better association results can indirectly help to other two sub-tasks in OVMOT. We provide the discussion and analysis of the complementarity among different tasks in Appendix 3.

#### 4.4 QUALITATIVE ANALYSIS

We conduct some qualitative analysis to more intuitively show the effect of our prompt-guided attention and the visualized comparison results of our method with the state-of-the-art algorithm.

**Illustrations of the proposed prompt-guided attention.** Figure 3 (a) shows cases of high prompt-guided attention, where we can see that the regions often have very distinctive category features, with no occlusion, and the image quality of the region is very high. In contrast, Figure 3 (b) presents cases of low prompt-guided attention, where we can observe that these regions often have issues such as heavy blurriness, occlusion, unclear visibility, and difficulty in identification. Such samples are very unsuitable for training the object localization and classification features, which are appropriately weakened through state-aware prompt-guided attention.

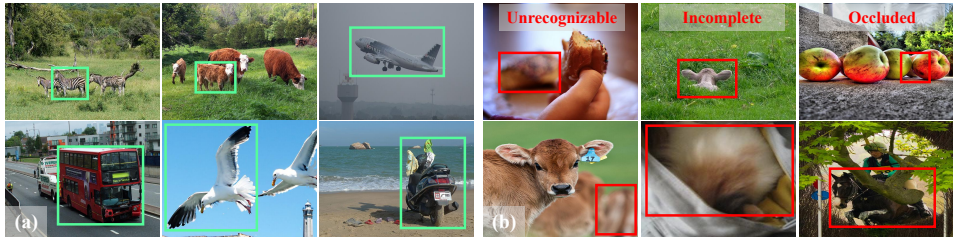


Figure 3: Illustration of regions with high (a) or low (b) prompt-guided attention, respectively.

**Comparison result visualization.** We show several visualization results in Figure 4. We can see that the proposed method provides better results than OVTrack (Li et al., 2023). In the first case of Figure 4 (a), our method provides an accurate object localization result and identifies the correct category. In the second case of Figure 4 (b), the tracking of a drone provided by the comparison method is wrong (different box colors denote different tracking IDs), also the classification is not correct. Our method can track it continuously. We also show some failure cases in Appendix 4.



Figure 4: Compared OVMOT results of ours and OVTrack on some cases with novel classes.

## 5 CONCLUSION

In this work, we have developed a new method namely VOVTrack to handle the OVMOT problem from the perspective of video object tracking. For this purpose, we first consider the object state during tracking and propose tracking-state-aware prompt-guided attention, which improves the accuracy of object localization and classification (detection). Second, we develop an object similarity learning strategy for the temporal association (tracking) using only the raw video data without annotation, which unveils the power of self-supervised learning for open-vocabulary tracking tasks. Experimental results demonstrate the effectiveness of the proposed method and each component for open-vocabulary tracking.

## REFERENCES

- Mykhaylo Andriluka, Stefan Roth, and Bernt Schiele. People-tracking-by-detection and people-detection-by-tracking. In *2008 IEEE Conference on computer vision and pattern recognition*, pp. 1–8. IEEE, 2008.
- Hexin Bai, Wensheng Cheng, Peng Chu, Juehuan Liu, Kai Zhang, and Haibin Ling. Gmot-40: A benchmark for generic multiple object tracking. In *Proceedings of the IEEE/CVF Conference on Computer Vision and Pattern Recognition*, pp. 6719–6728, 2021.
- Ankan Bansal, Karan Sikka, Gaurav Sharma, Rama Chellappa, and Ajay Divakaran. Zero-shot object detection. In *Proceedings of the European conference on computer vision (ECCV)*, pp. 384–400, 2018.
- Philipp Bergmann, Tim Meinhardt, and Laura Leal-Taixe. Tracking without bells and whistles. In *Proceedings of the IEEE/CVF international conference on computer vision*, pp. 941–951, 2019.
- Erik Bochinski, Volker Eiselein, and Thomas Sikora. High-speed tracking-by-detection without using image information. In *2017 14th IEEE international conference on advanced video and signal based surveillance (AVSS)*, pp. 1–6. IEEE, 2017.
- Jiarui Cai, Mingze Xu, Wei Li, Yuanjun Xiong, Wei Xia, Zhuowen Tu, and Stefano Soatto. Memot: Multi-object tracking with memory. In *Proceedings of the IEEE/CVF Conference on Computer Vision and Pattern Recognition*, pp. 8090–8100, 2022.
- Achal Dave, Pavel Tokmakov, and Deva Ramanan. Towards segmenting anything that moves. In *Proceedings of the IEEE/CVF International Conference on Computer Vision Workshops*, 2019.
- Achal Dave, Tarasha Khurana, Pavel Tokmakov, Cordelia Schmid, and Deva Ramanan. Tao: A large-scale benchmark for tracking any object. In *Computer Vision—ECCV 2020: 16th European Conference, Glasgow, UK, August 23–28, 2020, Proceedings, Part V 16*, pp. 436–454. Springer, 2020.
- Patrick Dendorfer, Hamid Rezaatofghi, Anton Milan, Javen Shi, Daniel Cremers, Ian Reid, Stefan Roth, Konrad Schindler, and Laura Leal-Taixé. Mot20: A benchmark for multi object tracking in crowded scenes. *arXiv preprint arXiv:2003.09003*, 2020.
- Akshay Dhamija, Manuel Gunther, Jonathan Ventura, and Terrance Boult. The overlooked elephant of object detection: Open set. In *Proceedings of the IEEE/CVF Winter Conference on Applications of Computer Vision*, pp. 1021–1030, 2020.

- Shuxiao Ding, Eike Rehder, Lukas Schneider, Marius Cordts, and Juergen Gall. 3dmotformer: Graph transformer for online 3d multi-object tracking. In *Proceedings of the IEEE/CVF International Conference on Computer Vision*, pp. 9784–9794, 2023.
- Thang Doan, Xin Li, Sima Behpour, Wenbin He, Liang Gou, and Liu Ren. Hyp-ow: Exploiting hierarchical structure learning with hyperbolic distance enhances open world object detection. In *Proceedings of the AAAI Conference on Artificial Intelligence*, volume 38, pp. 1555–1563, 2024.
- Fei Du, Bo Xu, Jiasheng Tang, Yuqi Zhang, Fan Wang, and Hao Li. 1st place solution to eccv-tao-2020: Detect and represent any object for tracking. *arXiv preprint arXiv:2101.08040*, 2021.
- Yu Du, Fangyun Wei, Zihe Zhang, Miaoqing Shi, Yue Gao, and Guoqi Li. Learning to prompt for open-vocabulary object detection with vision-language model. In *Proceedings of the IEEE/CVF Conference on Computer Vision and Pattern Recognition*, pp. 14084–14093, 2022.
- Yunhao Du, Zhicheng Zhao, Yang Song, Yanyun Zhao, Fei Su, Tao Gong, and Hongying Meng. Strongsort: Make deepsort great again. *IEEE Transactions on Multimedia*, 2023.
- Wei Feng, Feifan Wang, Ruize Han, Yiyang Gan, Zekun Qian, Junhui Hou, and Song Wang. Unveiling the power of self-supervision for multi-view multi-human association and tracking. *IEEE Transactions on Pattern Analysis and Machine Intelligence*, 2024.
- Tobias Fischer, Thomas E Huang, Jiangmiao Pang, Linlu Qiu, Haofeng Chen, Trevor Darrell, and Fisher Yu. Qdtrack: Quasi-dense similarity learning for appearance-only multiple object tracking. *IEEE Transactions on Pattern Analysis and Machine Intelligence*, 2023.
- Andreas Geiger, Philip Lenz, and Raquel Urtasun. Are we ready for autonomous driving? the kitti vision benchmark suite. In *Conference on Computer Vision and Pattern Recognition (CVPR)*, 2012.
- Xiuye Gu, Tsung-Yi Lin, Weicheng Kuo, and Yin Cui. Open-vocabulary object detection via vision and language knowledge distillation. In *International Conference on Learning Representations*, 2022.
- Agrim Gupta, Piotr Dollar, and Ross Girshick. Lvis: A dataset for large vocabulary instance segmentation. In *Proceedings of the IEEE/CVF conference on computer vision and pattern recognition*, pp. 5356–5364, 2019.
- Kuan-Chih Huang, Ming-Hsuan Yang, and Yi-Hsuan Tsai. Delving into motion-aware matching for monocular 3d object tracking. In *Proceedings of the IEEE/CVF International Conference on Computer Vision*, pp. 6909–6918, 2023.
- KJ Joseph, Salman Khan, Fahad Shahbaz Khan, and Vineeth N Balasubramanian. Towards open world object detection. In *Proceedings of the IEEE/CVF conference on computer vision and pattern recognition*, pp. 5830–5840, 2021.
- Jan Krejčí, Oliver Kost, Ondřej Straka, and Jindřich Duník. Pedestrian tracking with monocular camera using unconstrained 3d motion model. *arXiv preprint arXiv:2403.11978*, 2024.
- Laura Leal-Taixé, Cristian Canton-Ferrer, and Konrad Schindler. Learning by tracking: Siamese cnn for robust target association. In *Proceedings of the IEEE conference on computer vision and pattern recognition workshops*, pp. 33–40, 2016.
- Siyuan Li, Martin Danelljan, Henghui Ding, Thomas E Huang, and Fisher Yu. Tracking every thing in the wild. In *European Conference on Computer Vision*, pp. 498–515. Springer, 2022.
- Siyuan Li, Tobias Fischer, Lei Ke, Henghui Ding, Martin Danelljan, and Fisher Yu. Ovtrack: Open-vocabulary multiple object tracking. In *Proceedings of the IEEE/CVF conference on computer vision and pattern recognition*, pp. 5567–5577, 2023.
- Yang Liu, Idil Esen Zulfikar, Jonathon Luiten, Achal Dave, Deva Ramanan, Bastian Leibe, Aljoša Ošep, and Laura Leal-Taixé. Opening up open world tracking. In *Proceedings of the IEEE/CVF Conference on Computer Vision and Pattern Recognition*, pp. 19045–19055, 2022.

- Jonathon Luiten, Tobias Fischer, and Bastian Leibe. Track to reconstruct and reconstruct to track. *IEEE Robotics and Automation Letters*, 5(2):1803–1810, 2020.
- Tim Meinhardt, Alexander Kirillov, Laura Leal-Taixe, and Christoph Feichtenhofer. Trackformer: Multi-object tracking with transformers. In *Proceedings of the IEEE/CVF conference on computer vision and pattern recognition*, pp. 8844–8854, 2022.
- Anton Milan, S Hamid Rezatofighi, Anthony Dick, Ian Reid, and Konrad Schindler. Online multi-target tracking using recurrent neural networks. In *Proceedings of the AAAI conference on Artificial Intelligence*, volume 31, 2017.
- Dennis Mitzel and Bastian Leibe. Taking mobile multi-object tracking to the next level: People, unknown objects, and carried items. In *Computer Vision—ECCV 2012: 12th European Conference on Computer Vision, Florence, Italy, October 7-13, 2012, Proceedings, Part V 12*, pp. 566–579. Springer, 2012.
- Aljoša Ošep, Alexander Hermans, Francis Engelmann, Dirk Klostermann, Markus Mathias, and Bastian Leibe. Multi-scale object candidates for generic object tracking in street scenes. In *2016 IEEE International Conference on Robotics and Automation (ICRA)*, pp. 3180–3187. IEEE, 2016.
- Aljoša Ošep, Wolfgang Mehner, Paul Voigtlaender, and Bastian Leibe. Track, then decide: Category-agnostic vision-based multi-object tracking. In *2018 IEEE International Conference on Robotics and Automation (ICRA)*, pp. 3494–3501. IEEE, 2018.
- Aljoša Ošep, Paul Voigtlaender, Mark Weber, Jonathon Luiten, and Bastian Leibe. 4d generic video object proposals. In *2020 IEEE International Conference on Robotics and Automation (ICRA)*, pp. 10031–10037. IEEE, 2020.
- Jiangmiao Pang, Linlu Qiu, Xia Li, Haofeng Chen, Qi Li, Trevor Darrell, and Fisher Yu. Quasi-dense similarity learning for multiple object tracking. In *Proceedings of the IEEE/CVF conference on computer vision and pattern recognition*, pp. 164–173, 2021.
- Zheng Qin, Sanping Zhou, Le Wang, Jinghai Duan, Gang Hua, and Wei Tang. Motiontrack: Learning robust short-term and long-term motions for multi-object tracking. In *Proceedings of the IEEE/CVF conference on computer vision and pattern recognition*, pp. 17939–17948, 2023.
- Alec Radford, Jong Wook Kim, Chris Hallacy, Aditya Ramesh, Gabriel Goh, Sandhini Agarwal, Girish Sastry, Amanda Askell, Pamela Mishkin, Jack Clark, et al. Learning transferable visual models from natural language supervision. In *International conference on machine learning*, pp. 8748–8763. PMLR, 2021.
- Shafin Rahman, Salman Khan, and Nick Barnes. Improved visual-semantic alignment for zero-shot object detection. In *Proceedings of the AAAI conference on artificial intelligence*, volume 34, pp. 11932–11939, 2020.
- Shaoqing Ren, Kaiming He, Ross Girshick, and Jian Sun. Faster r-cnn: Towards real-time object detection with region proposal networks. *Advances in neural information processing systems*, 28, 2015.
- Amir Sadeghian, Alexandre Alahi, and Silvio Savarese. Tracking the untrackable: Learning to track multiple cues with long-term dependencies. In *Proceedings of the IEEE international conference on computer vision*, pp. 300–311, 2017.
- Fatemeh Saleh, Sadegh Aliakbarian, Hamid Rezatofighi, Mathieu Salzmann, and Stephen Gould. Probabilistic tracklet scoring and inpainting for multiple object tracking. In *Proceedings of the IEEE/CVF conference on computer vision and pattern recognition*, pp. 14329–14339, 2021.
- Piyush Sharma, Nan Ding, Sebastian Goodman, and Radu Soricut. Conceptual captions: A cleaned, hypernymed, image alt-text dataset for automatic image captioning. In *Proceedings of the 56th Annual Meeting of the Association for Computational Linguistics (Volume 1: Long Papers)*, pp. 2556–2565, 2018a.



- Sarthak Sharma, Junaid Ahmed Ansari, J Krishna Murthy, and K Madhava Krishna. Beyond pixels: Leveraging geometry and shape cues for online multi-object tracking. In *2018 IEEE International Conference on Robotics and Automation (ICRA)*, pp. 3508–3515. IEEE, 2018b.
- Vivek Hari Sridhar, Dominique G Roche, and Simon Gingins. Tracktor: image-based automated tracking of animal movement and behaviour. *Methods in Ecology and Evolution*, 10(6):815–820, 2019.
- Peize Sun, Jinkun Cao, Yi Jiang, Rufeng Zhang, Enze Xie, Zehuan Yuan, Changhu Wang, and Ping Luo. Transtrack: Multiple object tracking with transformer. *arXiv preprint arXiv:2012.15460*, 2020.
- Peize Sun, Jinkun Cao, Yi Jiang, Zehuan Yuan, Song Bai, Kris Kitani, and Ping Luo. Dancetrack: Multi-object tracking in uniform appearance and diverse motion. In *Proceedings of the IEEE/CVF Conference on Computer Vision and Pattern Recognition*, pp. 20993–21002, 2022.
- Li Wang, Xinyu Zhang, Wenyuan Qin, Xiaoyu Li, Jinghan Gao, Lei Yang, Zhiwei Li, Jun Li, Lei Zhu, Hong Wang, et al. Camo-mot: Combined appearance-motion optimization for 3d multi-object tracking with camera-lidar fusion. *IEEE Transactions on Intelligent Transportation Systems*, 2023.
- Zhongdao Wang, Jingwei Zhang, Liang Zheng, Yixuan Liu, Yifan Sun, Yali Li, and Shengjin Wang. Cycas: Self-supervised cycle association for learning re-identifiable descriptions. In *Computer Vision—ECCV 2020: 16th European Conference, Glasgow, UK, August 23–28, 2020, Proceedings, Part XI 16*, pp. 72–88. Springer, 2020.
- Nicolai Wojke, Alex Bewley, and Dietrich Paulus. Simple online and realtime tracking with a deep association metric. In *2017 IEEE international conference on image processing (ICIP)*, pp. 3645–3649. IEEE, 2017.
- Xiaoshi Wu, Feng Zhu, Rui Zhao, and Hongsheng Li. Cora: Adapting clip for open-vocabulary detection with region prompting and anchor pre-matching. In *Proceedings of the IEEE/CVF conference on computer vision and pattern recognition*, pp. 7031–7040, 2023.
- Bin Xiao, Haiping Wu, and Yichen Wei. Simple baselines for human pose estimation and tracking. In *Proceedings of the European conference on computer vision (ECCV)*, pp. 466–481, 2018.
- Alireza Zareian, Kevin Dela Rosa, Derek Hao Hu, and Shih-Fu Chang. Open-vocabulary object detection using captions. In *Proceedings of the IEEE/CVF Conference on Computer Vision and Pattern Recognition*, pp. 14393–14402, 2021.
- Fangao Zeng, Bin Dong, Yuang Zhang, Tiancai Wang, Xiangyu Zhang, and Yichen Wei. Motr: End-to-end multiple-object tracking with transformer. In *European Conference on Computer Vision*, pp. 659–675. Springer, 2022.
- Yifu Zhang, Chunyu Wang, Xinggang Wang, Wenjun Zeng, and Wenyu Liu. Fairmot: On the fairness of detection and re-identification in multiple object tracking. *International Journal of Computer Vision*, 129:3069–3087, 2021.
- Yiwu Zhong, Jianwei Yang, Pengchuan Zhang, Chunyuan Li, Noel Codella, Liunian Harold Li, Luowei Zhou, Xiyang Dai, Lu Yuan, Yin Li, et al. Regionclip: Region-based language-image pretraining. In *Proceedings of the IEEE/CVF Conference on Computer Vision and Pattern Recognition*, pp. 16793–16803, 2022.
- Kaiyang Zhou, Jingkang Yang, Chen Change Loy, and Ziwei Liu. Conditional prompt learning for vision-language models. In *Proceedings of the IEEE/CVF conference on computer vision and pattern recognition*, pp. 16816–16825, 2022a.
- Kaiyang Zhou, Jingkang Yang, Chen Change Loy, and Ziwei Liu. Learning to prompt for vision-language models. *International Journal of Computer Vision*, 130(9):2337–2348, 2022b.
- Xingyi Zhou, Vladlen Koltun, and Philipp Krähenbühl. Tracking objects as points. In *European conference on computer vision*, pp. 474–490. Springer, 2020.

Xingyi Zhou, Rohit Girdhar, Armand Joulin, Philipp Krähenbühl, and Ishan Misra. Detecting twenty-thousand classes using image-level supervision. In *European Conference on Computer Vision*, pp. 350–368. Springer, 2022c.

Xingyi Zhou, Tianwei Yin, Vladlen Koltun, and Philipp Krähenbühl. Global tracking transformers. In *Proceedings of the IEEE/CVF Conference on Computer Vision and Pattern Recognition*, pp. 8771–8780, 2022d.

## A APPENDIX

### APPENDIX 1. OVMOT PROBLEM

OVMOT requires the tracker to be capable of tracking objects from the open-vocabulary categories of objects. We first present the problem formulation of this task from the training and testing stages.

At training stage, the training data is  $\{\mathbf{X}^{\text{train}}, \mathcal{A}^{\text{train}}\}$  that contains video sequences  $\mathbf{X}^{\text{train}}$  and their respective annotations  $\mathcal{A}^{\text{train}}$  of the objects. Given one frame in the video, each annotation  $\alpha \in \mathcal{A}^{\text{train}}$  consists of a 2D bounding box  $\mathbf{b} = [x, y, w, h]$ , a unified ID  $d$  over the whole video, and a category label  $c$ , where  $(x, y)$  is the center pixel coordinates and  $(w, h)$  is the width and height of the box, the category belongs to the *base class* set, *i.e.*,  $c \in \mathcal{C}^{\text{base}}$ .

At the testing stage, the inputs consist of video sequences  $\mathbf{X}^{\text{test}}$  and the set of all object classes  $\mathcal{C} = \mathcal{C}^{\text{base}} \cup \mathcal{C}^{\text{novel}}$ , where  $\mathcal{C}^{\text{novel}}$  denotes the novel categories not appearing in the training set, *i.e.*,  $\mathcal{C}^{\text{novel}} \cap \mathcal{C}^{\text{base}} = \emptyset$ . OVMOT aims to obtain the trajectories of all objects in  $\mathbf{X}^{\text{test}}$  belonging to classes  $\mathcal{C}$ . Each trajectory  $\tau$  consists of a series of tracked objects  $\tau_t$  at frame  $t$ , and each  $\tau_t$  is composed of a 2D bounding box  $\mathbf{b}$ , and its object category  $c$ . Note that, during the testing stage, we need to evaluate not only the results on the base class  $\mathcal{C}^{\text{base}}$ , but also on the novel class  $\mathcal{C}^{\text{novel}}$ . The results on  $\mathcal{C}^{\text{novel}}$  can validate the tracker’s capability when facing objects from the open-vocabulary categories.

### APPENDIX 2. TRAINING DATA ANALYSIS

As discussed above, we use the training dataset in TAO for association module training. Next, we will analyze our experimental results from the perspective of the data quantity used for training.

**TAO dataset.** As shown in the first row of Table 3, we can see that the original TAO dataset has very few annotated frames, with only 18.1k frames, and limited box annotations of 54.7k. This is because the annotations in TAO were made at 1 FPS, resulting in a very limited number of supervised frames and available annotations for training a robust tracker.

As shown in the next row, in our self-supervised method, we use all the raw video frames without requiring any annotations. We can see that the usable frame quantity has increased to 30 times compared to the original training set (with annotations). Also, the quantity of available object bounding boxes for self-supervised training has reached 399.9k, which is 7.5 times the original number of annotated ones. Moreover, by integrating the long-short-term sampling strategies, we can fully utilize all the long-short-term frames within in the TAO raw videos through our self-supervised method, thereby achieving better results.

Table 3: The number of frames and annotations can be used to train in LVIS, annotated TAO, TAO in our self-supervised paradigm and CC3M.

Datasets	Frames		Annotations (detections)	
TAO (Original training set)	18.1k		54.7k	
TAO (Our self-supervision)	534.1k		399.9k	
Datasets	Frames		Annotations (detections)	
LVIS	base	novel	base	novel
	99.3k	1.5k	1264.9k	5.3k
Datasets	Frames		Annotations (captions)	
CC3M	3318.3k		3318.3k	

We further discuss the results using the training datasets of LVIS and CC3M.

**LVIS dataset.** As shown in Table 1 in the main paper, the comparison methods QDTrack (Fischer et al., 2023) and TETer (Li et al., 2022) trained on the LVIS dataset with both base and novel classes, still yield poor results in TAO validation and test sets. This may be due to the imbalance in the data quantity of base and novel categories. Specifically, as seen in Table 3, although the LVIS dataset has a large number of frames and annotations for its base classes, the data for its novel classes is very limited, with the number of frames being  $\frac{1}{66}$  and the number of annotations even less, at  $\frac{1}{239}$ .

**CC3M dataset.** We also list the data quantity of CC3M (Sharma et al., 2018a) in the last row of Table 3 to explain why our classification accuracy is slightly lower than the methods trained CC3M. We can see that the CC3M dataset is significantly larger, nearly 33 times the size of LVIS and 184 times that of TAO. In it, each frame caption also provides an average of about 10 words for training. The scenes and categories in the CC3M dataset are far more diverse than those in LVIS and TAO, which enables it to encounter a wider range of categories and achieve higher classification accuracy. However, it is noteworthy that, despite this, our method surpasses the results of the methods using CC3M in most metrics except classification, effectively demonstrating the effectiveness of our method.

### APPENDIX 3. MODULE COMPLEMENTARITY ANALYSIS

When designing the entire framework, we also consider the complementarity of the localization, association, and association modules, enabling them to assist each other.

**Improving classification via association.** Following the baseline (Li et al., 2023), we use the most frequently occurring category within a trajectory as the category for all objects in that trajectory. This approach indirectly improves classification results through better associations. Such assistance explains the reason that category clustering operations in our self-supervised object association training effectively increase classification accuracy, as shown in Table 2 in the main paper.

**Improving localization via association.** Additionally, during the association process, some candidates from the localization module with low detection confidence scores are retained because their association similarity surpasses the threshold. This association similarity priority strategy ensures that valid targets are retained, which improves the accuracy of localization.

Similarly, better localization and classification results also help achieve improved association results, making our entire framework a cohesive entirety with multiple modules working collaboratively.

### APPENDIX 4. FAILURE CASE ANALYSIS

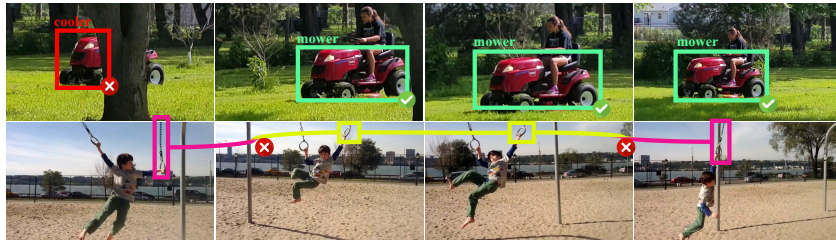


Figure 5: Failure case illustration.

We provide some failure cases in Figure 5. The first case illustrates a classification mistake due to significant occlusion. The second case shows the tracking errors caused by the distraction of object similarity and variability. We find that the OVMOT combined with the localization, classification, and tracking tasks has a significant challenge, yet it holds large research potential.

### APPENDIX 5. MORE DETAILS IN THE PROPOSED METHOD

**Details during training.** As mentioned in the main paper regarding the experimental procedure, compared to using the existing Open-Vocabulary Detection (OVD) method (Du et al., 2022) directly for localization and classification in OVTrack (Li et al., 2023), we train the OVD process using the base classes of the LVIS dataset and incorporate tracking-related states into the training process (Section 3.2). This significantly enhanced the localization and classification results in open-vocabulary object tracking.

Additionally, in the training of the association module, different from our baseline method (Li et al., 2023) using the generated image pairs constructed by LVIS, we further introduce a self-supervised method for object similarity learning (Section 3.3). Specifically, we utilize all the video frames in the TAO (Dave et al., 2020) training dataset for self-supervised training, which makes full use of the consistency among the objects in a video sequence and greatly improves the association task results.

**Long-Short-Interval Sampling Strategy.** We consider the interval splitting of  $\mathcal{T}_c$  in Eq. (4). As shown in Figure 6, we split the original videos into several segments of length  $L$  and randomly sample the shorter sub-segments with various lengths from each segment. These short-term sub-segments are then concatenated to form the training sequence. Such training sequences include long-short-term intervals. Specifically, we select the adjacent frames from the same sub-segment, which allow the association head to learn the consistency objectives under minor object differences. We also select the long-interval video frames from different sub-segments, which allow the association head to learn the similarity and variation of objects under large differences.

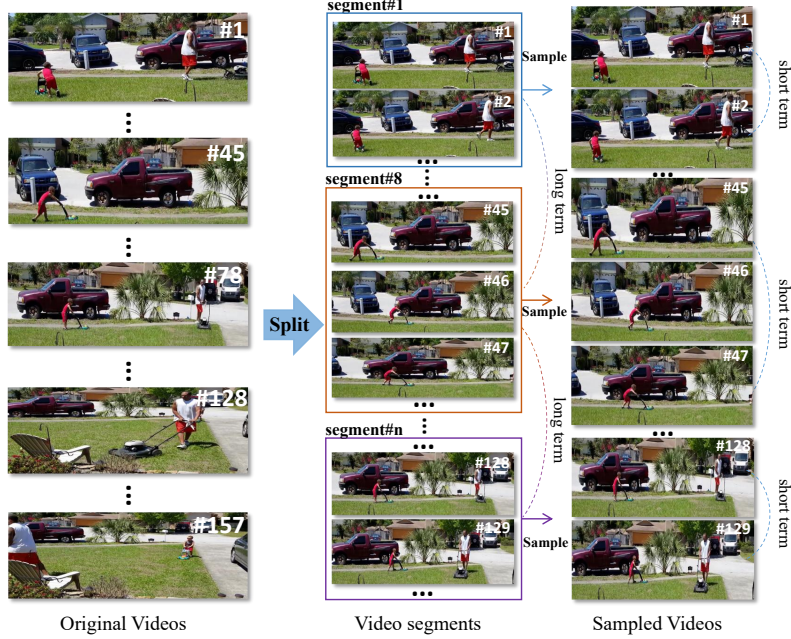


Figure 6: An illustration of interval sampling strategy.

**Metrics.** First, the localization accuracy (LocA) is determined through the alignment of all labeled boxes  $\alpha$  with the predicted boxes of  $\mathcal{T}$  without considering classification:  $\text{LocA} = \frac{|\text{TPL}|}{|\text{TPL}| + |\text{FPL}| + |\text{FNL}|}$ . Next, classification accuracy (ClsA) is calculated using all accurately localized TPL instances, by comparing the predicted semantic classes with the corresponding ground truth classes  $\text{ClsA} = \frac{|\text{TPC}|}{|\text{TPC}| + |\text{FPC}| + |\text{FNC}|}$ . Finally, association accuracy (AssocA) is determined using a comparable approach, by matching the identities of associated ground truth instances with accurately localized predictions  $\text{AssocA} = \frac{1}{|\text{TPL}|} \sum_{b \in \text{TPL}} \frac{|\text{TPA}(b)|}{|\text{TPA}(b)| + |\text{FPA}(b)| + |\text{FNA}(b)|}$ . The TETA score is computed as the mean value of the above three scores  $\text{TETA} = \frac{\text{LocA} + \text{ClsA} + \text{AssocA}}{3}$ .